Published in final edited form as:
Nanomedicine. 2010 April ; 6(2): 382–390. doi:10.1016/j.nano.2009.10.001.

Tumor-Associated Macrophages Are Predominant Carriers of Cyclodextrin-Based Nanoparticles into Gliomas

Darya Alizadeh, MS[1], **Leying Zhang, PhD**[1], **Jungyeon Hwang, PhD**[2], **Thomas Schluep, ScD**[2], and **Behnam Badie, MD**[1]

[1] Division of Neurosurgery, City of Hope National Cancer Center, 1500 East Duarte Road, Duarte, CA 91010

[2] Calando Pharmaceuticals, 129 N. Hill Ave, Suite 104, Pasadena, CA 91107

Abstract

The goal of this study was to evaluate the mechanism of cyclodextrin-based nanoparticle (CDP-NP) uptake into a murine glioma model. Using mixed *in vitro* culture systems, we demonstrated that CDP-NP was preferentially taken up by BV2 and N9 microglia (MG) cells as compared to GL261 glioma cells. Fluorescent microscopy and flow cytometry analysis of intracranial (i.c.) GL261 gliomas confirmed these findings and demonstrated a predominant CDP-NP uptake by macrophages (MP) and MG within and around the tumor site. Interestingly, in mice bearing bilateral i.c. tumor, MG and MP carrying CDP-NP were able to migrate to the contralateral tumors. In conclusion, these studies better characterize the cellular distribution of CDP-NP in i.c. tumors and demonstrate that MP and MG could potentially be used as nanoparticle drug carriers into malignant brain tumors.

Keywords

Nanoparticle; brain neoplasm; central nervous system; and microglia

Introduction

Treatment of malignant brain tumors continues to challenge scientists and clinicians alike. Location of these tumors within the central nervous system (CNS), which is considered a “privileged” organ, can prevent the penetration of chemotherapeutic agents through the blood-brain barrier (BBB) (1). Furthermore, recently-developed targeted macromolecules are unable to effectively penetrate through tight junctions that constitute an intact and otherwise healthy BBB. As a result, new drug delivery technologies are being developed to circumvent this obstacle (2,3).

Use of nanoparticles (NPs) as drug carriers has received significant attention recently (4). Polymer based NPs have many advantages such as high systemic bioavailability, attenuation of early drug degradation, less toxicity, and high solubility. Complex macromolecules can be

Corresponding Author: Behnam Badie, MD, Division of Neurosurgery, 1500 East Duarte Road, Duarte, CA 91010, Phone: (626) 471-7100, Fax: (626) 471-7344, bbadie@coh.org.

Conflict of Interest Statement: The senior author owns stocks in Arrowhead Research Inc, which is a part owner of Calando Pharmaceuticals.

designed to carry not only therapeutic drugs, but also ligands that could preferentially bind and target specific receptors on tumor cells. It is thought that extravasation of these molecules through an abnormal tumor vasculature, in addition to specific surface ligands, can potentially lead to higher local drug concentrations and uptake in tumors. Although this hypothesis has been proven to be correct in a number of tumor models (5), penetration of these macromolecules through an intact BBB could hinder their uptake by tumors located in the CNS. To overcome this limitation, nanoparticles are either covered by tumor specific ligands or delivered directly into the CNS using convention-enhanced or bulk-flow delivery techniques (4,6). Another delivery technique that has not been as well studied is the uptake and transport of nanoparticles by tumor stromal cells such as tumor-associated macrophages (TAMs).

In contrast to traditionally accepted notion that the BBB restricts penetration of inflammatory cells into the CNS, it is now believed that continuous surveillance of CNS tissue is taking place by both resident microglia (MG) and migrating lymphocytes (7). Furthermore, under pathological conditions, such as inflammation, autoimmune diseases, and cancers, immune-competent cells and monocytes can readily cross the disrupted BBB to participate in repair or exacerbate injury (8).

Arising from both resident brain MG and circulating monocytes, TAMs represent a significant component of inflammatory response to gliomas (9–12). In CNS inflammatory conditions, activated MG and MP release pro-inflammatory cytokines and become capable of phagocytosis and antigen presentation (8). Several studies have also confirmed an intact MP phagocytic function in gliomas (13,14). These findings suggest that TAMs are still capable of phagocytosis and could potentially be employed as nanoparticle carriers into brain tumors.

In this study we characterized the uptake and distribution of cyclodextrin-based NP (CDP-NP) into glioma models. Although the pharmacokinetics and biodistribution of this polymer conjugated to camptothecin has been studied in systemic cancer(15), little information is available about its uptake by intracranial (i.c.) tumors. Considering the phagocytic properties of MG and MP, we hypothesized that TAM could act as carriers of NP into intracranial tumors. Here, we report efficient CDP-NP uptake by MG *in vitro* and by TAM *in vivo*. Furthermore, i.c. injections of CDP-NP resulted in polymer uptake by TAM and their migration into the circulation and even distant tumor sites within the CNS. Efficient uptake of CDP-NP by TAM and their distribution to multifocal tumors supports the use of TAM as NP carriers for treatment of malignant brain tumors.

Materials and Methods

Cell Culture and Tumor Model

Mouse microglia BV2, and N9 cell lines were obtained from ATCC. GL261, murine glioma cell line, was stably transfected with firefly luciferase and eGFP expression vectors and positive clones (GL261-ffluci and GL261-eGFP) were selected using zeocin (1mg/ml) and G418, respectively incubated in DMEM supplemented with 10% fetal bovine serum (FBS), penicillin (100 U/ml), and streptomycin (100 μg/ml). All cell lines were cultured at 37°C in a humidified 5% CO_2 atmosphere.

Animal studies were approved by the City of Hope Research Animal Care Committee. All animals were housed and handled in accordance with humane guidelines implemented by this committee. Intracranial tumor implantation was performed as described previously with modifications (16). GL261-ffluci or GL261-eGFP cells were harvested by trypsinization, counted, and resuspended in 0.1 M PBS. C57BL/6 mice (Jackson Laboratory, Bar Harbor, ME, USA) weighing 15–25 g were anesthetized by intraperitoneal (i.p.) administration of ketamine (132mg/kg) and xylazine (8.8mg/kg), and immobilized in a stereotactic head frame. Through

a small burr hole, 3 μl of PBS containing 1 × 105 tumor cells was injected unilaterally or bilaterally at the coronal suture, 1 mm lateral to the midline and 3 mm deep into the frontal lobes, using a Hamilton syringe (Fisher Scientific, Pittsburgh, PA, USA).

Synthesis of CDP-Rhodamine Nanoparticles

A linear, beta-cyclodextrin-based polymer containing free thiol groups (CDP-SH) was prepared as previously described (17). CDP-SH (100 mg, 0.022 mmol) was dissolved in nano pure water (2 ml). Rhodamine Red® C2 maleimide (Invitrogen, Carlsbad, CA) (15 mg, 0.022 mmol) in DMSO (1 mL) was added to the polymer solution and stirred for 4 h. N-ethylmaleimide (28 mg, 0.22 mmol) was then added and stirred for additional ½ h. The mixture was diluted with nano pure water to the volume of 60 ml. The solution was dialyzed using 25,000 molecular weight cutoff MWCO membrane (Spectra/Por 7, Spectrum Labs, Rancho Dominguez, CA) for 24 h. It was filtered through 0.2 μm filters (Nalgene, Rochester, NY) and lyophilized to yield purple solid (78mg, 67% Yield). Particle size and zeta potential was measured on a Zeta PALS instrument (Brookhaven Instrument Corporation, Holtsville, NY). Particle size of CDP-Rhodamine in water was 69.7 nm. Zeta potential of CDP-Rhodamine in 40 mM HEPES at pH 7.4 was measured to be 3.91 ± 0.57 mV.

Biophotonic Tumor Imaging

Tumor-bearing animals were injected with luciferin (4.29 mg/mouse) and anesthetized animals were imaged with the Xenogen IVIS *In Vivo* Imaging System (Xenogen, Palo Alto, CA, USA). Luciferase activity was analyzed using Living Image Software (Xenogen, Palo Alto, CA, USA) to quantify tumor region flux (photons per second) and to confirm tumor growth before animals were used for *in vivo* studies.

Optical imaging

Animals bearing two-week old GL261-eGFP gliomas were injected intravenously (through tail vein) (i.v., 100mg/kg) or intratumorally (i.t., 1mg/kg) with CDP-NP conjugated with Rhodamine. Twenty-four hours later, anesthetized mice were perfused with ice-cold PBS followed by paraformaldehyde (4%). Brains were harvested, sectioned into 100 micron-thick slices with a Vibratome (Vibratome, St. Louis, MO, USA), and imaged using a Leica Z16 Macrofluar Fluorescent Macroscope (Leica Microsystems Inc., Bannockburn, IL, USA). Ten micron slides were also imaged using a Zeiss LSM 510 Meta inverted 2-photon confocal microscope (Leica Microsystems Inc., Bannockburn, IL, USA) with 20x and 63x objective lens.

Flow Cytometry

Mice bearing two-week old tumors were given i.v. (100mg/kg) or i.t. (1mg/kg) injections of Rhodamine-conjugated CPD-NP. At various time intervals, animals were euthanized and tumors, spleen, and blood samples were harvested for flow cytometry. Cell suspensions from normal brain (NB), GL261ffluci tumors, and spleen were forced through a 40 μm filter. Spleen and blood samples were incubated in Gey's buffer (pH 7.2) for 10 min. All samples were washed twice, and resuspended in 0.1 M PBS containing 1% FBS and 2mM EDTA (18). All antibodies (Abs) and isotype controls were purchased from BD Biosciences (San Jose, CA, USA) or eBiosciences (San Diego, CA, USA). Fluorescein isothiocyanate (FITC) conjugated anti-mouse CD11b (clone M1/70) and Allophycocyanin (APC)-conjugated anti-mouse CD45 (clone 30-F11) Abs were used at a dilution of 1:300 and 1:400, respectively. Samples were incubated with the appropriate primary Ab or isotype controls for 1 h at 4°C. Cells were then washed and isolated using the MoFlo fluorescence cell sorter (BDIS, San Jose, CA, USA). Lasers used were one Argon laser set at 488 nm excitation for FITC collection (530/30 filter), one krypton laser set at 647 nm excitation for APC collection (680/30 filter), and a second

krypton laser set at 568 nm excitation for collection of Rhodamine Red (600/30 filter). FlowJo 8.5.3 software was used for data analysis. Tumor-associated cells labeled as $CD45^{hi}$/$CD11b^{+}$ were designated as MP, $CD45^{low}$/$CD11b^{+}$ as MG, and $CD45^{+}$/$CD11b^{-}$ as lymphocytes as described before (18).

Results

CDP-NP synthesis and characterization

A linear, cyclodextrin-based polymer (CDP) was fluorescently labeled by covalently attaching rhodamine through a maleimide linker and quenching any remaining unreacted free sulfhydryl groups with N-ethylmaleimide. The resulting polymer conjugate self-assembled to nanoparticles (CDP-NP) with similar characteristics to IT-101, a CDP conjugate with camptothecin currently in clinical development (Table 1). Important characteristics of CDP-NP are a particle size between 10 nm and 100 nm, near neutral surface charge (zeta potential $< \pm 10$ mV), and high water solubility (> 100 mg/mL).

CDP-NP internalization by microglia and glioma cell lines

In order to compare the efficacy of CDP-NP uptake by glioma and MG, mixed culture of GL261-eGFP and BV2 cells were incubated with CDP-NP (0.1mg/ml) for 0, 6, 12, or 48 h. Samples were collected at the end of each time-point and analyzed by flow cytometry (Figure 1). CDP-NP appeared to be internalized by both cell types, but the uptake rate as measured by both CDP-NP-positive cells (Figure 1A) and mean fluorescent intensity (Figure 1B) appeared to be higher in BV2 MG cells. By 48 h, however, 90% of each cell type was positive for CDP-NP. Fluorescent microscopy confirmed that CDP-NP was in fact internalized by cells and not bound to cell membrane (Figure 1C). Similar observations were made with N9 MG cell line (data not shown).

CDP-NP uptake by intracranial gliomas

To assess CDP-NP uptake by gliomas, mice bearing intracranial GL261-eGFP gliomas were injected i.v. with CDP-NPs. Twenty-four hours later, brains were harvested and imaged by fluorescent microscopy. In normal mice, Rhodamine signal was only visible along the perivascular spaces and choroid plexus (not shown). But in tumor-bearing animals, CDP-NPs were also visualized within and at the edges of the tumors (Figure 2A). Interestingly, high-power images showed that most of the CDP-NP internalization appeared to be by non-glioma cells located at the tumor edge (Figure 2B). CDP-NP uptake by tumor-associated cells may have been due to migration of NP-positive circulating cells into tumors, NP extravasation through blood-tumor barrier and subsequent uptake by resident stromal cells, or both processes. To understand this mechanism, we studied the phenotypes of CDP-NP-positive cells by flow cytometry.

Microglia and macrophage uptake of CDP-Rho particles in vivo

To determine which cell types preferentially internalized CDP-NP *in vivo*, mice bearing two-week old i.c. tumors were injected with CDP-NP i.v. (100mg/kg) or i.t. (1mg/kg). Flow cytometry was used to analyze CDP-NP uptake by four cell populations discussed in the methods section (Figure 3). Irrespective of route of administration, CDP-NP uptake appeared to be more pronounced by TAM (MG and MP) as these cells accounted for approximately 60–80% of NP-positive cells in i.c. gliomas (Figure 4 A and B). Interestingly, MG appeared to be as active as MP in CDP-NP uptake, and as expected, internalized CDP-NP more efficiently when the particles were injected directly into tumors as compared to systemically (Figure 4 C and D). In addition, mice injected i.v. demonstrated stable levels of CDP-NP-positive MP and MG over four days (Figure 4C). Conversely, i.t. injected mice showed a decrease in the level

of both cell populations that was most pronounced for the MP on day 4 (Figure 4D). Since CDP-NP-positive MP was detected in blood and spleen (not shown) after i.t. injection, it suggests possible trafficking of MP in and out of the brain. Overall, these findings validate the *in vitro* observations and suggest that the phagocytic properties of MG and MP (as part of their innate immune function) may be intact and responsible for efficient CDP-NP uptake in this glioma model.

To further elucidate the migratory properties of CPD-NP-positive cells in this model, blood (Figure 5) and spleen (not shown) samples were also analyzed by flow cytometry. As expected, a significant population of CPD-NP-positive cells was detected in each organ after i.v. injections. The distribution of these cells was not dependent on their CD11b expression, suggesting that both lymphocytes and monocytes were equally capable of carrying the NP. Interestingly following i.t. injections, the majority of CPD-NP-positive cells expressed high levels of CD11b even after 4 days (Figure 5). Because very few lymphocytes (CD45+) were NP-positive in i.t. injected group, this observation indicates that the NP-positive cells were monocytic cells that originated from the tumor tissue and not circulating monocytes that took up extravasated CDP-NP. These results, once again, demonstrate the monocytes' ability to uptake and carry NP to and from brain tumors. Whether similar migratory properties were present in the CNS was studied next.

Migration of CDP-NP positive cells in the CNS

In order to determine if the MG/MP population can migrate within the CNS, mice bearing bilateral GL261 tumors were generated and injected i.t. unilaterally. Tumor samples were removed from injected (ipsilateral) and contralateral hemispheres and studied for CDP-NP uptake (Figure 6). Consistent with the previous experiments, TAM accounted for most of the CDP-NP-positive cells even seven days after CDP-NP injections. Interestingly, within 24 h of i.t. injection, approximately 75% of MG cells and 50% of MP in the contralateral tumor were found to be CDP-NP-positive suggesting their migration within the CNS. Strong contralateral TAM labeling was less likely due to CDP-NP extravasation into CNS or intravascular space because: 1) The proportion of nonspecific labeling of tumor-associated cells due to leakage of CDP-NP at the time of injection (zero-time) was minimal when only 15–20% of cells were NP-positive (Figure 6), and 2) Although uptake of extravasated CDP-NP by circulating monocytes (prior to migration to the contralateral tumor) could partially account for NP-positive TAM, this is unlikely because only 10% of circulating monocytes were NP-positive at day 4 after i.t. injections (Figure 4D). Thus, these results strongly suggest that both MG and MP are capable of migration within the CNS and could potentially carry NP to distant tumor sites.

Discussion

Nanoparticle-mediated drug delivery is receiving increasing attention for treatment of cancer (19). Drugs bound to NPs may be resistant to first-time metabolism and excretion or deactivation by tumor cells. Furthermore, it has been suggested that because of their size, NPs effectively pass through tumor microvessels, thus leading to higher intratumoral concentrations. Although it is generally assumed that NPs are taken up by tumor cells, their cellular biodistribution in brain tumors has not been studies in detail. Moreover, presence of the BBB may provide another obstacle for their effective uptake and distribution in CNS tumors. To address these issues, we evaluated the cellular biodistribution of CDP-NPs in an i.c. glioma model. The CDP-NPs are currently being studied as camptothecin carriers in human trials (15,20). In order to be able to detect CDP-NPs *in vivo*, we attached the fluorescent label rhodamine instead of camptothecin to the same parent polymer. This substitution resulted in nanoparticles with similar key characteristics such as particle size, surface charge and

solubility, making it a good if not a perfect model system. Here we demonstrate several interesting observations that may apply to other NP delivery systems: First, irrespective of route of administration (i.v. vs. i.c.), CDP-NPs were more efficiently taken up by TAM (MP and MG) than tumor cells. Second, TAMs not only phagocytized NPs but also were able to migrate into the circulation after local i.c. CDP-NP injections. And finally, NP-positive TAMs distributed to distant tumors within the CNS after local i.c. delivery (Figure 6). Overall, these results support further investigation into the application of TAMs as NP carriers for treatment of malignant brain tumors.

Although, the exact biological function of TAM in malignant brain tumors is still unclear, studies have suggested both pro and anti-neoplastic phenotypes (21). In support of an intact MG/MP innate immune function, depletion of MG/MP from tumor models has been shown to result in tumor progression in mouse GL261 gliomas (22). Others have also demonstrated that TAMs are capable of phagocytosis suggesting an active innate function. Hussain *et al*. demonstrated active phagocytosis of beads by MP isolated from fresh GBM samples *ex vivo* (13). Similarly, Nickles *et al* showed phagocytosis of apoptotic glioma cells by activated MP *in vitro* (14). Our findings also suggest that TAM can efficiently phagocytize foreign particles, possibly indicating an intact pro-inflammatory function. Other studies, however, have suggested that TAM's innate function may be suppressed in gliomas. TAMs in rodent gliomas are more resistant to toll-like receptor (TLR) activation as compared to MG and MP in normal brains; perhaps due to the local immunosuppressive micro-environment (23). Indeed, exposure to tumor-derived factors such as IL-4, IL-10, hyaluronic acid, TGF-β, M-CSF, is believed to induce TAMs to differentiate into "alternatively activated" MP (also known as M2 MP) in other tumor models (24). M2 cells are thought to contribute to tumor progression and invasion by secreting growth, angiogenic, and immunosuppressive factors (25–28). Although these observations have been mainly reported in non-glial tumors such as breast and lung cancers, recent studies suggest that similar mechanisms may be present in malignant gliomas (29,30). Using immunohistochemistry, Komohara *et al.* reported strong expression of M2 markers, CD163 and CD204, on MG/MP in high-grade gliomas (29). Additionally, recent gene expression analysis of tumor specimens have demonstrated upregulation of genes associated with M2 cells (30). Overall, these findings suggest that although TAMs can phagocytize NPs and can be activated outside of tumor microenvironment, they appear to have M2 characteristics *in vivo*, lack effective antineoplastic functions and may even support glioma growth (31,32). Despite an unclear biological role in gliomas, the ability of TAMs to uptake NPs can be exploited to develop therapeutic approaches to increase the anti-neoplastic functions of TAMs for better treatment of brain tumors.

Although early studies demonstrated active uptake of iron NP by gliomas (33), the exact cellular distribution of NP within tumors was not addressed until recently. When assessing quantum dots for intra-operative glioma localization, Jackson *et al.* noted that the majority of NP were in fact taken up by TAMs (34). In a similar study evaluating uptake dynamics of CLIO-Cy5.5 (NPs containing a superparamagnetic iron oxide core coated with Cy5.5-labeled dextran), Trehin *et al.* noted that nearly 21% of the NP were engulfed by TAMs following i.v. injections (35). In the case of CDP-NP, the current study also highlights the significant contribution of TAMs in NP uptake and delivery into brain tumors. This information can be important when designing NP-based treatments for brain tumors in several ways: First, NP uptake by TAMs may allow for selective modulation and stimulation of these cells in gliomas, potentially enhancing their antitumor innate function. For example, NPs can be developed to activate TAMs through either engaging TLR receptors (36), or suppressing the inhibitory pathways (such as Stat3) that have been proposed to play a role in tumor immune evasion (37,38). Second, there may be variability in TAM infiltration and function between glioma models and human tumors, thus leading to inconsistent findings when animal NP uptake and function studies are extrapolated to human trials. Furthermore, the role of NP shuttling by

TAMs is unknown for other types of cancers where free NPs in plasma may play a larger role in their biodistribution. Third, efficient uptake of NPs, in general, by TAMs and circulating monocytes can result in rapid NP clearance, consequently decreasing their biodistribution into tumors. Because CDP-NP serum concentrations were not measured in this study, the contribution of NP shuttling to the overall CDP-NP bio-availability can not be deduced in this study. Previous human studies with similar CDP-NPs, however, have shown the presence of large circulating pools of free CDP-NP in plasma, indicating that both cell-associated and free NP may circulate for extended periods of time within the vascular space (39). Finally, monocytes have been reported to have defects in base excision repair mechanisms and are more sensitive to methylating agents such as temozolomide and cisplatin which are commonly used for glioma therapy (40). Therefore, when NPs are used for delivery of cytotoxic agents, selective depletion of monocytes may exacerbate immunosuppression in patients with brain tumors. Although this may be a limitation when CDP-NP are being used to brain cancer therapy, the same approach may be useful for depletion of monocytes in the treatment of non-neoplastic inflammatory conditions such as encephalitis or radiation-induced inflammation (41).

The ability of TAMs to migrate in and out of i.c. tumors and to circulate and distribute to other tumors within the CNS, highlights another potential application of NP for treatment of malignant brain tumors. In contrast to previously held notion that the brain is an “immune privileged” organ, there is now evidence demonstrating intact afferent and efferent immune pathways in normal and inflamed CNS tissue (7). Migration of MP and monocytes into brain tissue has also been demonstrated previously (42), Valable *et al.* were able to noninvasively image migration of labeled monocytes and MP into i.c. gliomas after their systemic administration (42). Although these authors could not image MP migration within the CNS by MRI, our findings in bilateral tumors strongly suggest that TAMs could potentially migrate between multiple i.c. tumors (Figure 6). This latter finding suggests that TAMs can be used to carry NPs into invasive or multifocal brain tumors.

In summary, we have reported efficient CDP-NP uptake by MG and MP in gliomas. Furthermore, i.c. injections of CDP-NP resulted in efficient polymer uptake by TAM and their migration into the circulation and even distant tumor sites within the CNS. These findings further support the use of TAM as NP carriers for treatment of malignant brain tumors. Future studies will focus on the use of NP for immune modulation of TAMs in brain tumor models.

Abbreviations

BBB	Blood Brain Barrier
CDP-NP	Cyclodextrin-based Nanoparticle
CNS	Central Nervous System
i.c	Intracranial
i.t	Intratumoral
i.v	Intravenous
MP	Macrophage
MG	Microglia
NP	Nanoparticle
TAMs	Tumor-associated macrophages

References

1. Muldoon LL, Soussain C, Jahnke K, Johanson C, Siegal T, Smith QR, et al. Chemotherapy delivery issues in central nervous system malignancy: a reality check. J Clin Oncol 2007 Jun 1;25(16):2295–305. [PubMed: 17538176]
2. Pardridge WM. Drug targeting to the brain. Pharmaceutical research 2007 Sep;24(9):1733–44. [PubMed: 17554607]
3. Patel MM, Goyal BR, Bhadada SV, Bhatt JS, Amin AF. Getting into the brain: approaches to enhance brain drug delivery. CNS drugs 2009;23(1):35–58. [PubMed: 19062774]
4. Jain KK. Use of nanoparticles for drug delivery in glioblastoma multiforme. Expert review of neurotherapeutics 2007 Apr;7(4):363–72. [PubMed: 17425491]
5. Byrne JD, Betancourt T, Brannon-Peppas L. Active targeting schemes for nanoparticle systems in cancer therapeutics. Advanced drug delivery reviews 2008 Dec 14;60(15):1615–26. [PubMed: 18840489]
6. Reimold I, Domke D, Bender J, Seyfried CA, Radunz HE, Fricker G. Delivery of nanoparticles to the brain detected by fluorescence microscopy. Eur J Pharm Biopharm 2008 Oct;70(2):627–32. [PubMed: 18577452]
7. Galea I, Bechmann I, Perry VH. What is immune privilege (not)? Trends Immunol 2007;28:12–8. [PubMed: 17129764]
8. Djukic M. Circulating monocytes engraft in the brain, differentiate into microglia and contribute to the pathology following meningitis in mice. Brain 2006;129:2394–403. [PubMed: 16891321]
9. Badie B, Schartner JM. Flow cytometric characterization of tumor-associated macrophages in experimental gliomas. Neurosurgery 2000 Apr;46(4):957–61. discussion 61–2. [PubMed: 10764271]
10. Roggendorf W, Strupp S, Paulus W. Distribution and characterization of microglia/macrophages in human brain tumors. Acta Neuropathologica 1996;92(3):288–93. [PubMed: 8870831]
11. Shinonaga M, Chang CC, Suzuki N, Sato M, Kuwabara T. Immunohistological evaluation of macrophage infiltrates in brain tumors. Correlation with peritumoral edema. J Neurosurg 1988;68 (2):259–65. [PubMed: 3276837]
12. Streit WJ. Cellular immune response in brain tumors. Neuropathology & Applied Neurobiology 1994;20(2):205–6. [PubMed: 8072665]
13. Hussain SF, Yang D, Suki D, Grimm E, Heimberger A. Innate immune functions of microglia isolated from human glioma patients. Journal of Translational Medicine 2006;4(1):15. [PubMed: 16573834]
14. Nickles D, Abschuetz A, Zimmer H, Kees T, Geibig R, Spiess E, et al. End-stage dying glioma cells are engulfed by mouse microglia with a strain-dependent efficacy. J Neuroimmunol 2008 Jul;197 (1):10–20. [PubMed: 18495256]
15. Schluep T, Cheng J, Khin KT, Davis ME. Pharmacokinetics and biodistribution of the camptothecin-polymer conjugate IT-101 in rats and tumor-bearing mice. Cancer chemotherapy and pharmacology 2006 May;57(5):654–62. [PubMed: 16133526]
16. VanHandel M, Alizadeh D, Zhang L, Kateb B, Bronikowski M, Manohara H, et al. Selective uptake of multi-walled carbon nanotubes by tumor macrophages in a murine glioma model. J Neuroimmunol 2009 Mar 31;208(1–2):3–9. [PubMed: 19181390]
17. Schluep T, Gunawan P, Ma L, Jensen GSJDSH, et al. Polymeric Tubulysin-Peptide Nanoparticles with Potent Antitumor Activity. Clin Cancer Res 2009;15(1):181–9. [PubMed: 19118045]
18. Badie B, Bartley B, Schartner J. Differential expression of MHC class II and B7 costimulatory molecules by microglia in rodent gliomas. J Neuroimmunol 2002 Dec;133(1–2):39–45. [PubMed: 12446006]
19. Brannon-Peppas L, Blanchette JO. Nanoparticle and targeted systems for cancer therapy. Advanced drug delivery reviews 2004 Sep 22;56(11):1649–59. [PubMed: 15350294]
20. Schluep T, Hwang J, Cheng J, Heidel JD, Bartlett DW, Hollister B, et al. Preclinical efficacy of the camptothecin-polymer conjugate IT-101 in multiple cancer models. Clin Cancer Res 2006 Mar 1;12 (5):1606–14. [PubMed: 16533788]
21. Watters JJ, Schartner JM, Badie B. Microglia function in brain tumors. Journal of neuroscience research 2005 Aug 1;81(3):447–55. [PubMed: 15959903]

22. Galarneau H, Villeneuve J, Gowing G, Julien JP, Vallieres L. Increased glioma growth in mice depleted of macrophages. Cancer research 2007 Sep 15;67(18):8874–81. [PubMed: 17875729]

23. Schartner JM, Hagar AR, Van Handel M, Zhang L, Nadkarni N, Badie B. Impaired capacity for upregulation of MHC class II in tumor-associated microglia. Glia 2005 Apr 7;51(4):279–85. [PubMed: 15818597]

24. Sica A, Bronte V. Altered macrophage differentiation and immune dysfunction in tumor development. J Clin Invest 2007 May;117(5):1155–66. [PubMed: 17476345]

25. Condeelis J, Pollard JW. Macrophages: obligate partners for tumor cell migration, invasion, and metastasis. Cell 2006 Jan 27;124(2):263–6. [PubMed: 16439202]

26. Lewis CE, Pollard JW. Distinct role of macrophages in different tumor microenvironments. Cancer research 2006 Jan 15;66(2):605–12. [PubMed: 16423985]

27. Pardoll D. Does the immune system see tumors as foreign or self? Annu Rev Immunol 2003;21:807–39. [PubMed: 12615893]

28. Sica A, Schioppa T, Mantovani A, Allavena P. Tumour-associated macrophages are a distinct M2 polarised population promoting tumour progression: potential targets of anti-cancer therapy. Eur J Cancer 2006 Apr;42(6):717–27. [PubMed: 16520032]

29. Komohara Y, Ohnishi K, Kuratsu J, Takeya M. Possible involvement of the M2 anti-inflammatory macrophage phenotype in growth of human gliomas. The Journal of pathology 2008 Apr 17;216:15–24. [PubMed: 18553315]

30. Murat A, Migliavacca E, Gorlia T, Lambiv WL, Shay T, Hamou MF, et al. Stem cell-related "self-renewal" signature and high epidermal growth factor receptor expression associated with resistance to concomitant chemoradiotherapy in glioblastoma. J Clin Oncol 2008 Jun 20;26(18):3015–24. [PubMed: 18565887]

31. Nishie A, Ono M, Shono T, Fukushi J, Otsubo M, Onoue H, et al. Macrophage infiltration and heme oxygenase-1 expression correlate with angiogenesis in human gliomas. Clin Cancer Res 1999 May; 5(5):1107–13. [PubMed: 10353745]

32. Wesolowska A, Kwiatkowska A, Slomnicki L, Dembinski M, Master A, Sliwa M, et al. Microglia-derived TGF-beta as an important regulator of glioblastoma invasion--an inhibition of TGF-beta-dependent effects by shRNA against human TGF-beta type II receptor. Oncogene 2008 Feb 7;27(7): 918–30. [PubMed: 17684491]

33. Zimmer C, Weissleder R, Poss K, Bogdanova A, Wright SC Jr, Enochs WS. MR imaging of phagocytosis in experimental gliomas. Radiology 1995 Nov;197(2):533–8. [PubMed: 7480707]

34. Jackson H, Muhammad O, Daneshvar H, Nelms J, Popescu A, Vogelbaum MA, et al. Quantum dots are phagocytized by macrophages and colocalize with experimental gliomas. Neurosurgery 2007 Mar;60(3):524–9. discussion 9–30. [PubMed: 17327798]

35. Trehin R, Figueiredo JL, Pittet MJ, Weissleder R, Josephson L, Mahmood U. Fluorescent nanoparticle uptake for brain tumor visualization. Neoplasia (New York, NY) 2006 Apr;8(4):302–11.

36. Carpentier, AF.; Tibi, A.; Richard, M.; Capelle, L.; Laigle-Donadey, F.; Behin, A., et al. Local Treatment with an immunostimulatory CpG-oligonucleotide in Patients with recurrent glioblastoma: Results of a phase I trial. Second quadrennial meeting of the World Federation of Neuro-Oncology; May 5–8, 2005; Edinburgh, UK. 2005.

37. Hussain SF, Kong LY, Jordan J, Conrad C, Madden T, Fokt I, et al. A novel small molecule inhibitor of signal transducers and activators of transcription 3 reverses immune tolerance in malignant glioma patients. Cancer research 2007 Oct 15;67(20):9630–6. [PubMed: 17942891]

38. Kortylewski M, Yu H. Role of Stat3 in suppressing anti-tumor immunity. Current opinion in immunology 2008 Apr;20(2):228–33. [PubMed: 18479894]

39. Yen Y, Synold T, Schluep T, Hwang J, Oliver M, Davis ME. First-in-human phase I trial of a cyclodextrin-containing polymer-camptothecin nanoparticle in patients with solid tumors. Journal of Clinical Oncology 2007;25(18S):14078.

40. Briegert M, Kaina B. Human monocytes, but not dendritic cells derived from them, are defective in base excision repair and hypersensitive to methylating agents. Cancer research 2007 Jan 1;67(1):26–31. [PubMed: 17210680]

41. Davoust N, Vuaillat C, Androdias G, Nataf S. From bone marrow to microglia: barriers and avenues. Trends in immunology 2008;29(5):227–34. [PubMed: 18396103]

42. Valable S, Barbier EL, Bernaudin M, Roussel S, Segebarth C, Petit E, et al. In vivo MRI tracking of exogenous monocytes/macrophages targeting brain tumors in a rat model of glioma. NeuroImage 2008 Apr 1;40(2):973–83. [PubMed: 18441552]

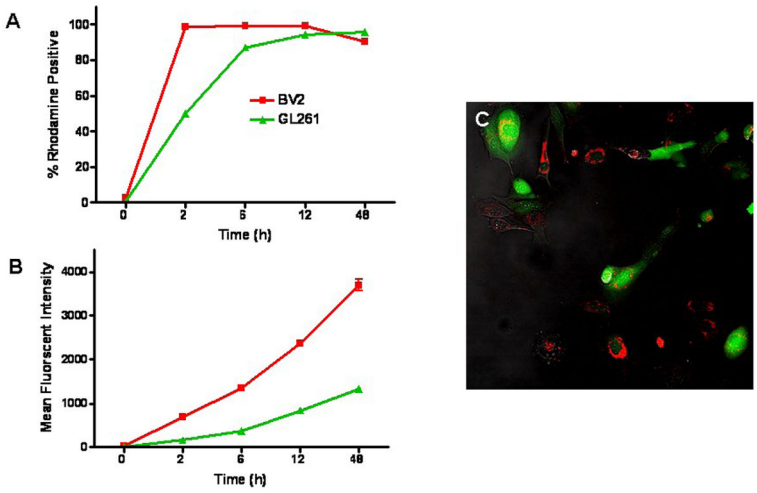

Figure 1. ***In vitro*** **uptake of CDP-NP by microglia and glioma cells**

CDP-NP internalization was assessed by flow cytometry (A and B) and confocal microscopy (C) in a mixed BV-2 and GL261-eGFP culture system incubated with CDP-NP (0.1 mg/ml). As determined by proportion of positive cells (A), and mean fluorescent intensity (B), BV2 microglia were more efficient in CDP-NP uptake as compared to GL261 glioma cells (Representative data ± SD from one of two separate experiments is shown, n=3 for each time-point). Fluorescent microscopy (C) confirmed that CDP-NPs (red particles) were internalized (and not surface bound) by both BV-2 and GL261-eGFP cells (green cells).

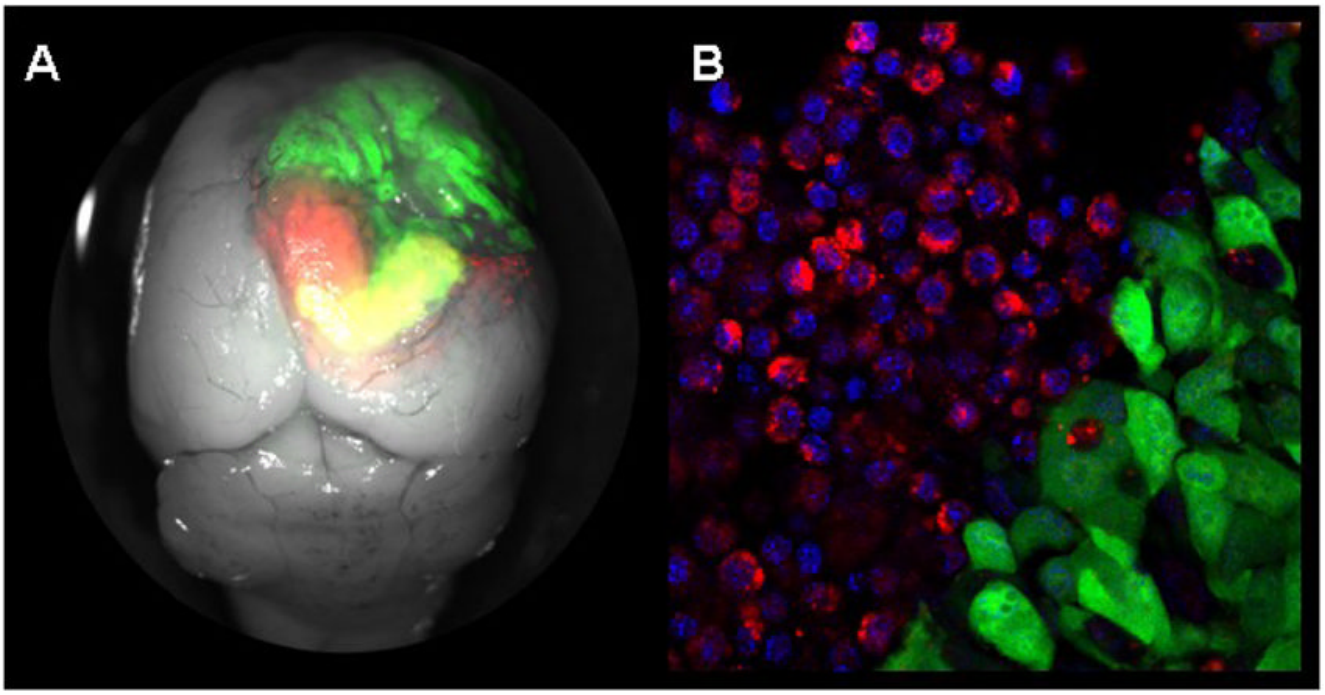

Figure 2. CDP-NP uptake by intracranial gliomas

Mice bearing intracranial GL261-eGFP gliomas were injected intravenously (i.v. 100mg/Kg) with CDP-NP (100mg/kg). Twenty-four h later, brains were harvested and imaged. A: Superimposed light and fluorescent microscopy images of the tumor-bearing brain demonstrating CDP-NP uptake (red fluorescent) by portions (yellow) of the tumor (green). B: High-power confocal microscopy showing that most of the CDP-NP uptake occurred by non-glial cells at the edge of the tumor (green fluorescent). Cell nuclei were stained with DAPI (63x objective).

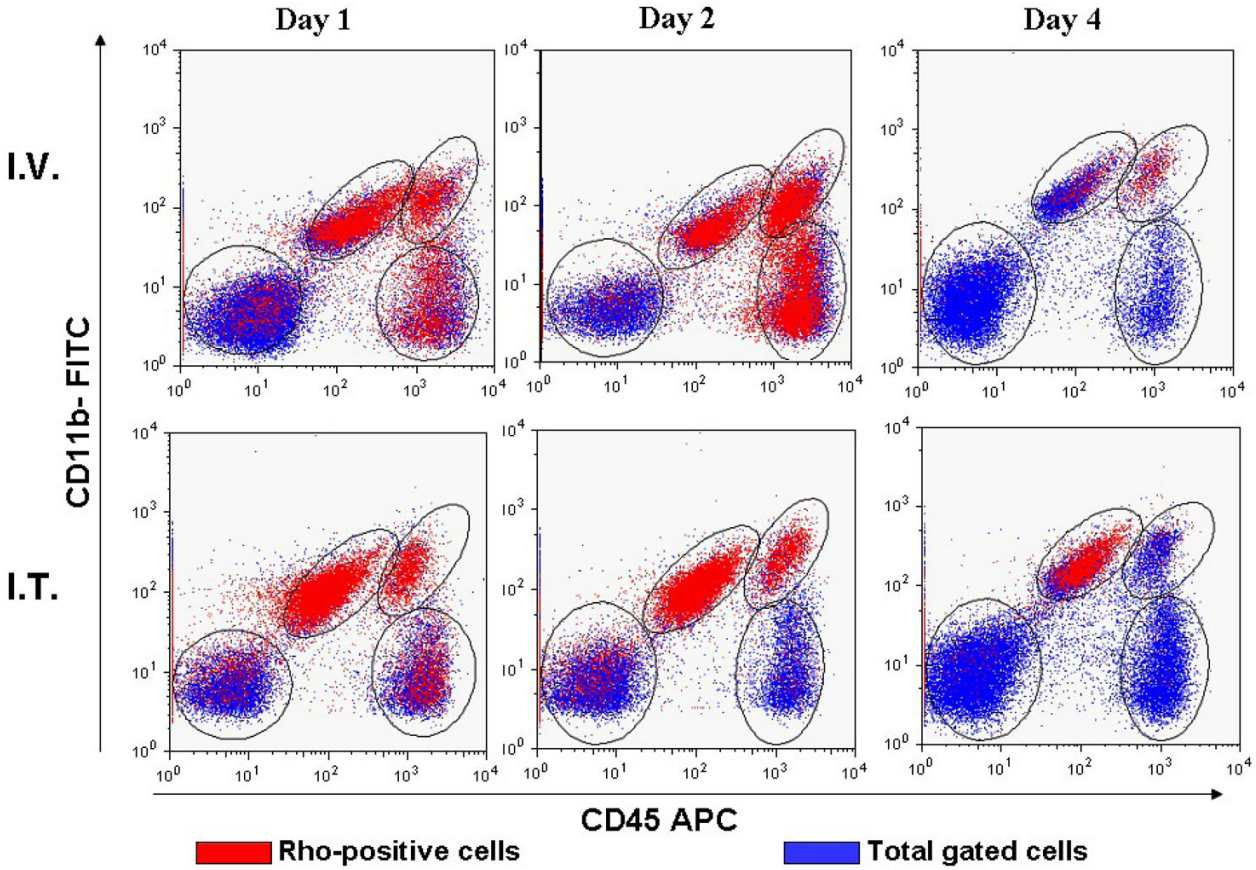

Figure 3. CDP-NPs are predominantly internalized by tumor-associated leukocytes

Flow cytometry was performed to identify CDP-NP-positive cells following intravenous (i.v., 100 mg/kg) or intratumoral (i.t., 1 mg/kg) injections. Representative dot plots demonstrating that the majority of CDP-NP uptake occurred by tumor macrophages (MP, $CD45^{hi}/CD11b^{+}$), microglia (MG,$CD45^{low}/CD11b^{+}$), and lymphocytes ($CD45^{+}/CD11b^{-}$). Representative histograms of two separate experiments are shown (n=3 animals/group).

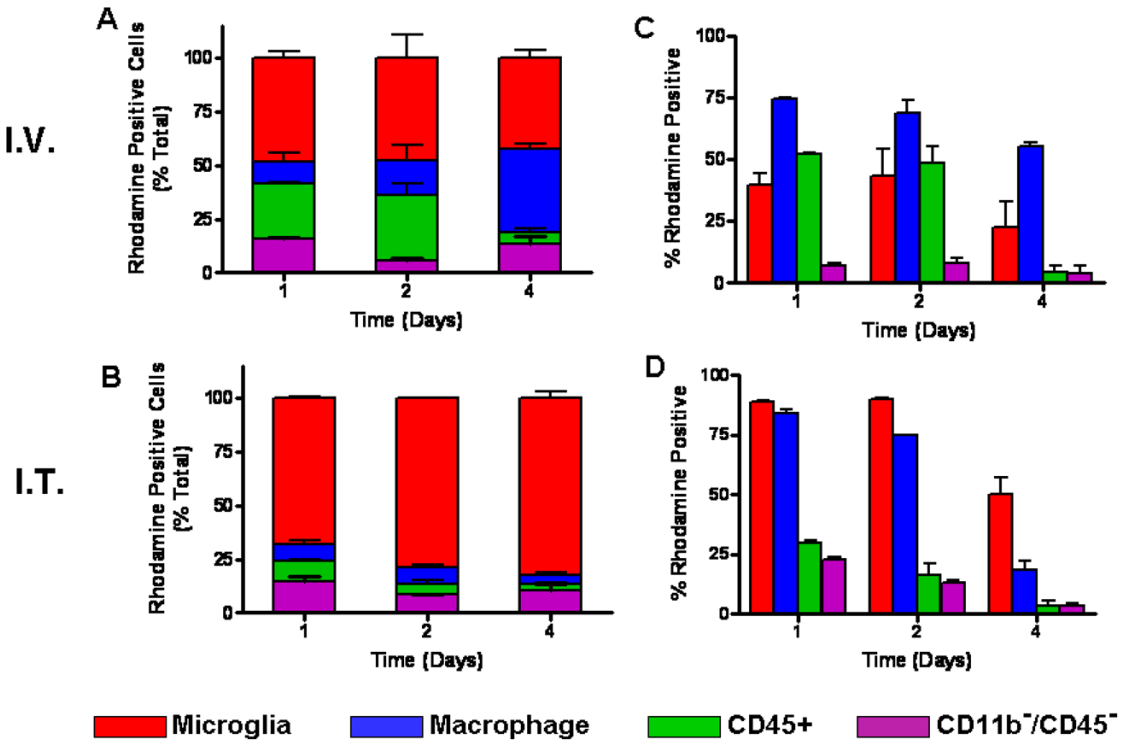

Figure 4. Quantification of CDP-NP uptake by tumor-associated leukocytes

The percentage of CDP-NP-positive cells by cell type (left panel) and the proportion of each cell type that internalized CDP-NPs (right panel) was determined after tumor-bearing animals were injected with NPs intravenously (i.v., 100mg/kg) or intratumorally (i.t., 1 mg/kg). Irrespective of route of administration, tumor-associated microglia (MG, $CD45^{low}/CD11b^{+}$) and macrophages (MP, $CD45^{hi}/CD11b^{+}$) accounted for most CDP-NP uptake (A and B). Furthermore, MG appeared to be as active as MP in CDP-NP uptake, but internalized CDP-NP more efficiently when the particles were injected directly into tumors as compared to systemically (C and D). Data is summarized as mean percent of Rhodamine-positive cells ± SD. Representative data of two separate experiments is shown (n=3 animals/group).

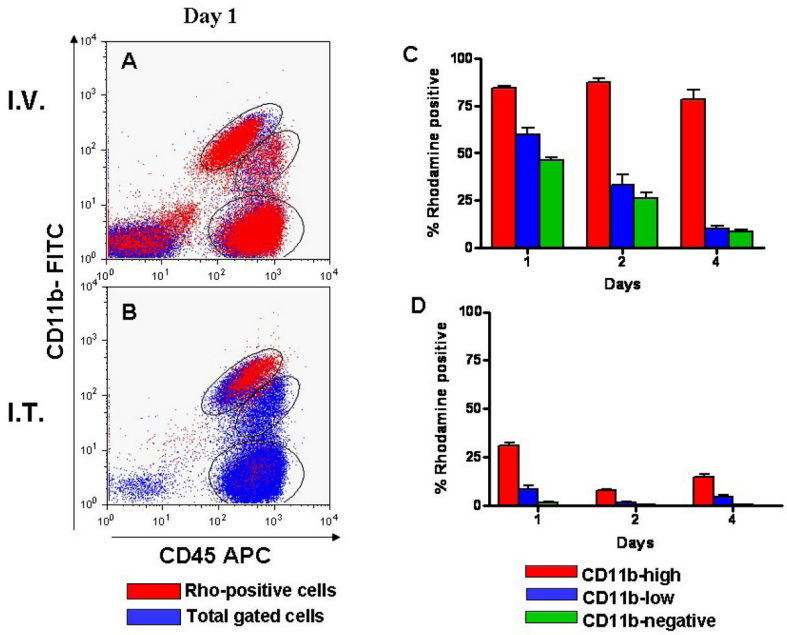

Figure 5. CDP-NP uptake in blood

Flow cytometry was performed to identify CDP-NP-positive cells following intravenous (i.v., 100 mg/kg) or intratumoral (i.t., 1 mg/kg) injections. Representative dot plots (A and B) demonstrating significant uptake of CDP-NP by circulating leukocytes after i.v. (A) and by monocytes after i.t. (B) injections. (C, D) Graphs representative of percent NP- positive cells in the blood. Blood CD45+CD11b+high NP positive were highest among the circulating luekocytes after intravenous (C) and intratumoral injections (D). Circulating monocytes ($CD45^{+}/CD11b^{high}$), accounted for the majority of NP-positive cells irrespective of route of administration. Data is summarized as mean percent of Rhodamine-positive cells ± SD. Representative data of two separate experiments is shown (n=3 animals/group).

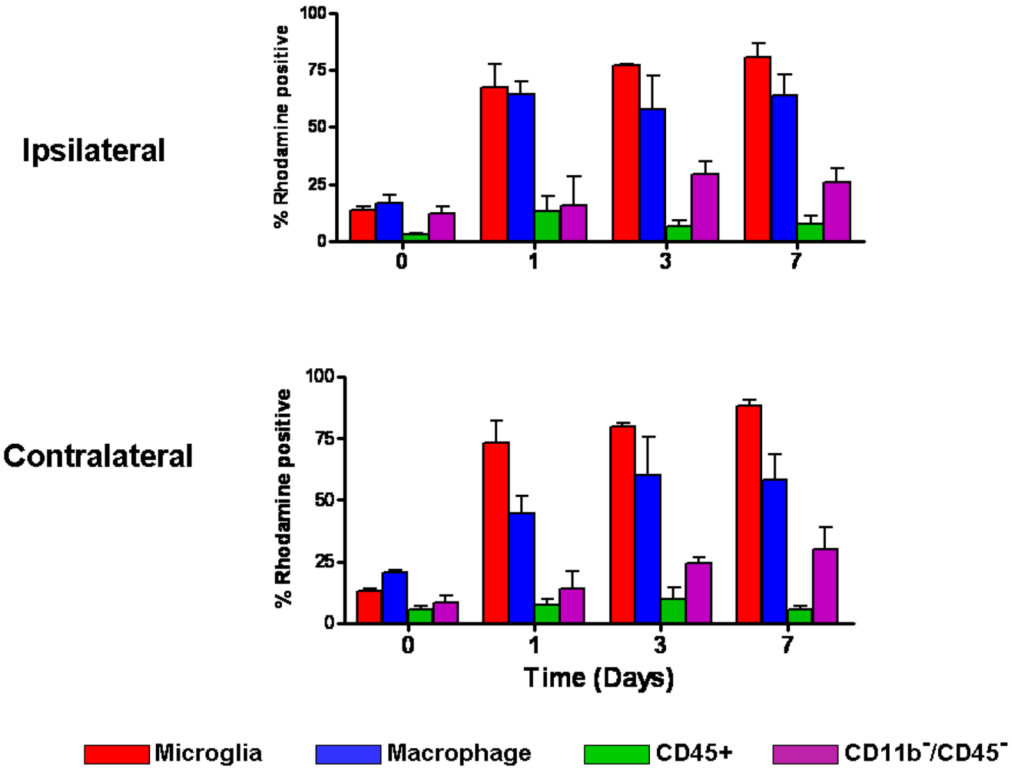

Figure 6. Migration of CDP-NP positive cells in the CNS

Mice bearing bilateral GL261 tumors received unilateral intratumoral (i.t. 1 mg/Kg) injections of CDP-NP (1 mg/kg). Tumor samples ipsilateral and contralateral to the injection site were removed and studied for CDP-NP uptake by flow cytometry. CDP-NP-positive Tumor-associated microglia ($CD45^{low}/CD11b^{+}$) and macrophages ($CD45^{hi}/CD11b^{+}$) were detected even after injection of NPs into the opposite hemisphere. Data is summarized as mean percent of Rhodamine-positive cells ± SD. Representative data of two separate experiments is shown (n=3 animals/group).

Table 1

Physico-chemical characteristics of CDP-Rhodamine nanoparticles compared to IT-101, a CDP-conjugate with camptothecin currently in clinical development.

Parameter	CDP polymer	CDP-CPT (IT-101)	CDP-Rhodamine
MW, PDI	67 kDa, 2.1	67 kDa, 2.1	67 kDa, 2.1
Camptothecin	n/a	9.2% w/w	n/a
Free Camptothecin	n/a	0.01%	n/a
Rhodamine	n/a	n/a	10% w/w
Free Rhodamine	n/a	n/a	None detected
Particle size	8 nm	36 nm	69.7 nm
Zeta potential	n/a	− 1.81 +/− 0.79 mV	3.91 +/− 0.57 mV
Solubility	>100 mg/mL	>100 mg/mL	>100 mg/mL